Simulating Canopy Transpiration and Photosynthesis of Corn Plants under Contrasting Water Regimes Using a Coupled Model

Y. Yang, S.-H. Kim, D. J. Timlin, D. H. Fleisher, B. Quebedeaux, V. R. Reddy

Abstract. *A process-based corn simulation model (MaizSim) was coupled with a two-dimensional soil simulator (2DSOIL) to simulate transpiration and photosynthesis of corn under contrasting water regimes. To improve the simulation of stomatal reaction to drought stress, a hydraulic stomatal control algorithm was implemented in the coupled photosynthesis-stomatal conductance module. Corn plants were grown in sunlit growth chambers and irrigated at three different frequencies. Simulated soil water content, transpiration, and photosynthesis rates were compared with those measured in the chambers. Comparison among simulations and measurements indicated that the coupled model was able to simulate the changes in soil water contents as well as the changes in transpiration and photosynthesis rates of corn plants under varying water status over the growing season. It was also found that the simulated photosynthesis rates were not as sensitive to reduction in stomatal conductance as the simulated transpiration rates. Reasons for this difference are discussed from the modeling viewpoint. This result agreed with the differences in sensitivity of photosynthesis and transpiration to changes in stomatal closure that have been reported in the literature. These results suggest that the coupled model not only is a valuable tool in studying corn transpiration and photosynthesis under drought stress, but it also provides a platform to implement and evaluate algorithms in studies of corn crop water dynamics and CO_2 assimilation.*

Keywords. *Crop modeling, Drought stress, Growth chamber, Soil water content, Stomatal conductance.*

Water acts as both a solvent for life-sustaining chemicals and as a structural component to provide form to a living organism. A common constraint to plant growth in agricultural ecosystems is lack of water. In order to accurately predict growth and yield of a plant under drought stress, a computer crop simulation model must be able to realistically quantify the reactions of different physiological processes to varying water status.

Both transpiration and photosynthesis occur through stomata of plant leaves. Stomatal conductance is affected by atmospheric conditions, such as irradiance, temperature, and water vapor pressure deficit, as well as soil water status. It is therefore crucial for a crop model to posses the ability to simulate stomatal conductance in reaction to environmental changes and soil drying. There are few models that are able to describe stomatal opening/closure mechanistically. The stomatal conductance models proposed by Ball et al. (1987) and Leuning (1995) are able to describe the dependence of stomatal conductance on net carbon assimilation, relative humidity, and leaf internal CO_2 concentration. These models have been widely accepted and applied (Aphalo and Jarvis, 1993; Dang et al., 1998; Lhomme et al., 1998). However, since the effect of soil water stress on stomatal conductance is not explicitly included in this type of model, there are often difficulties in simulating the change in stomatal conductance in a wide range of soil water regimes (Gao et al., 2002).

As demonstrated by Tuzet et al. (2003), simulation of stomatal conductance must be incorporated into a comprehensive model of photosynthesis, leaf energy balance, and water flow from soil through the plant to the atmosphere. To adopt this approach, the mechanism through which stomatal conductance is linked to varying soil water status has to be addressed. Hydraulic signals have been documented in response to wounding at the leaf level (Malone and Stankovic, 1991; Jones, 1998) or in affecting stomatal width as a function of cell turgor (Cowan, 1977; Wei et al., 1999). It has also been reported that closure of stomata of *Zea mays* (Hirasawa and Hsiao, 1999; Grams et al., 2007) and bell pepper plants (Yao et al., 2001) was induced by hydraulic signals.

Williams et al. (1996), Gao et al. (2002), and Jensen et al. (2000) simulated stomatal conductance as a direct function of soil water potential. Buckley and Mott (2002) and Leuning et al. (2003) suggested that leaf water potential controls stomatal conductance. Tuzet et al. (2003) proposed a model that coupled stomatal conductance, photosynthesis, leaf energy balance, and transport of water through the soil-plant-atmosphere continuum. In the model, leaf water potential,

Submitted for review in December 2007 as manuscript number BE 7314; approved for publication by the Biological Engineering Division of ASABE in March 2009.

The authors are **Yang Yang, ASABE Member Engineer,** Research Associate, Wye Research and Education Center, University of Maryland, Queenstown, Maryland; **Soo Hyung Kim,** Assistant Professor, College of Forest Resources, University of Washington, Seattle, Washington; **Dennis J. Timlin,** Soil Scientist, and **David H. Fleisher, ASABE Member Engineer,** Agricultural Engineer, USDA-ARS Crop Systems and Global Change Laboratory, Beltsville, Maryland; **Bruno Quebedeaux,** Professor, Department of Plant Sciences and Landscape Architecture, University of Maryland, College Park, Maryland; and **Vangimalla R. Reddy,** Plant Physiologist and Research Leader, USDA-ARS Crop Systems and Global Change Laboratory, Beltsville, Maryland. **Corresponding author:** Yang Yang, Wye Research and Education Center, P.O. Box 169, Queenstown, MD 21658-0169; phone: 410-827-8056; fax: 410-827-9039; e-mail: yang.yang@ars.usda.gov.

which was a function of soil water potential, controlled the closure of stomata under drought stress. However, as indicated by the authors, the model was not yet validated by experimental evidence, and the model did not separate the canopy into sunlit/shaded leaves, nor did the model consider the development of a crop under drought stress. Furthermore, it used a single, homogeneous soil layer with a uniform root distribution.

A process-based corn simulation model (MaizSim) has been developed by the USDA-ARS Crop System and Global Change Laboratory (CSGCL) at Beltsville, Maryland, to simulate corn growth and development as a function of key environmental variables. The model adopts the biochemical C_4 photosynthesis model (Von Caemmerer, 2000) and the BWB paradigm of stomatal conductance (Ball et al., 1987) to simulate stomatal conductance, photosynthesis, and transpiration of a corn plant. The BWB stomatal conductance module in the model does not incorporate a mechanism for the physiological control involved in root-shoot signaling under drought stress. Therefore, research is needed to improve the model's ability to simulate transpiration and photosynthesis of corn under drought stress. The 2DSOIL model is a modular, comprehensive two-dimensional soil simulator that is specifically designed to be combined with existing plant models (Timlin et al., 1996). Modules of 2DSOIL can simulate water, solute, heat, and gas movement, as well as root activity of plants in a two-dimensional soil profile that is partitioned into multiple layers. Coupling the MaizSim model with 2DSOIL provides a soil-plant-atmosphere continuum system that possesses the potential of taking into account the information of dynamic soil water status in simulating corn transpiration and photosynthesis.

The objectives of this study are: (1) to construct a coupled MaizSim+2DSOIL model that is capable of simulating changes in soil moisture levels and the transpiration and photosynthesis of corn plants under varying soil water status, and (2) to evaluate the performance of the coupled model by comparing the simulated transpiration and photosynthesis with those measured from corn plants under different soil water regimes.

Materials and Methods

The Model

The new model is constructed by coupling MaizSim with 2DSOIL, a two-dimensional finite element model describing water flow and heat transport. In the coupled model, MaizSim is responsible for simulating the potential transpiration demand as a function of light, temperature, humidity, CO_2, and wind velocity, while 2DSOIL determines actual water uptake rate in respond to the transpiration demand and soil water content (fig. 1).

In MaizSim, canopy transpiration and photosynthesis are simulated using the sun/shade method, which splits the big-leaf model into sunlit and shaded fractions (De Pury and Farquhar, 1997). The sun/shade model divides the canopy into sunlit and shaded fractions and models each fraction separately with a single-layer model. The sun/shade approach is able to incorporate canopy features such as the penetration of beam irradiance, its variation through the day, and the range of leaf angles in a canopy of uniform leaf angle distribution. Since the sunlit and shaded leaf fractions change during the day with solar elevation, the irradiance absorbed by the sunlit and shaded leaf fractions changes, too (De Pury and Farquhar, 1997; Mercado et al., 2006).

At the leaf level, the biochemical model of C_4 photosynthesis by Von Caemmerer (2000), the BWB stomatal conductance model and its variation that simulates stomatal closure in relation to soil drying, and an energy balance model (Kim and Lieth, 2003) are combined together to simulate leaf transpiration and photosynthesis (see Appendix A). The coupled model uses daily weather data (radiation, max-min temperature, and mean relative humidity) as input but scales the data to an hourly time interval (Timlin et al., 2002).

Leaf stomatal conductance is simulated with the BWB model and a variant of the BWB model that incorporates stomatal closure mechanism into the BWB model. Figure 2 describes the interaction among environmental variables and stomatal conductance simulated by the original BWB model and the modified BWB model.

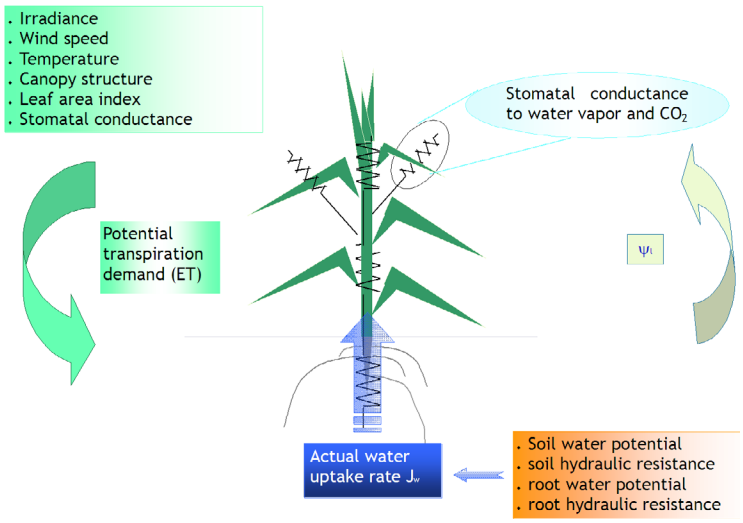

Figure 1. Schematic description of the coupled model in calculating potential transpiration rate and actual water uptake in each time step. In MaizSim, potential transpiration rate is affected by atmospheric condition as well as stomatal conductance to water vapor. Actual water uptake rate is determined in 2DSOIL by soil moisture level as well as soil-plant-atmosphere hydraulic conductivity. Information regarding soil water status is passed back to MaizSim in terms of hydraulic signal (leaf water potential, ψ_l).

$$g_s = g_0 + mA\frac{h_s}{(C_s / P_a)} f(\ ) \quad (1)$$

where g_0 is minimum stomatal conductance to water vapor at the light compensation point in the BWB model (= 0.0960 mol m^{-2} s^{-1}; Kim and Lieth, 2003); A is net CO_2 assimilation rate (μmol m^{-2} s^{-1}); m is an empirical coefficient for the sensitivity of g_s to A, C_s and h_s; C_s is CO_2 partial pressure at the leaf surface (μbar); and h_s is relative humidity at the leaf surface (Collatz et al., 1991).

$$C_s = C_a - A\frac{1.37}{g_b}P_a \quad (2)$$

$$a_h h_s^2 + b_h h_s + c_h = 0$$

$$\text{where } \begin{cases} a_h = (g_1 A)/C_s \\ b_h = g_0 + g_b - (g_1 A / C_s) \\ c_h = (-h_a g_b) - g_0 \end{cases} \quad (3)$$

Function $f(\psi)$ in the model describes the stomatal closure controlling mechanism in regard to leaf water status. The function can take different forms. In the original BWB model, since stomatal conductance is not controlled through any hydraulic signals (the "no-control" algorithm), $f(\psi)$ = 1. When it is assumed that stomatal closure is mainly controlled by hydraulic signal (the "control-by-psil" algorithm), the function can take the following form (Tuzet et al., 2003):

$$f_1(\psi_l) = \frac{1+\exp[s_f \psi_f]}{1+\exp[s_f(\psi_f - \psi_l)]} \quad (4)$$

where ψ_l is bulk leaf water potential, ψ_f is a reference potential (= –1.2 MPa), and s_f is a sensitivity parameter (= 2.3) (Tuzet et al., 2003). Performance of the coupled models with and without stomatal controlling mechanisms will be evaluated by comparing the simulated and measured transpiration and photosynthesis rates of corn plants under contrasting soil water content.

After the transpiration demand is determined by MaizSim, the water uptake and root growth module, developed by Acock and Trent (1991) for soybean and adopted into 2DSOIL, calculates the bulk leaf water potential necessary to satisfy the transpiration demand at the current soil moisture level. The water uptake and root growth module in Acock and Trent (1991) applied the general principles of osmotic adjustment and water diffusion in simulating root water uptake. Because of the generality of the principles, the functions can be used in simulations for other crops (Timlin et al., 1996).The actual soil-to-leaf water uptake is then described as an Ohm's law analog:

$$J_w = \frac{\psi_s - \psi_l}{R_{sr} + R_r + R_z} \quad (5)$$

where ψ_s is soil water potential, R_{sr} is soil to root hydraulic resistance, R_r is root hydraulic resistance, and R_z is xylem hydraulic resistance. Values and calculations of R_{sr} and R_r followed Timlin et al. (1996), and R_z is assumed to be a constant (= 0.149e3 m^2 s MPa/mol H_2O; Dewar, 2002).

Experiment

The measured data used for analysis in this article were acquired from an unpublished experiment in which corn response to CO_2 enrichment and drought was studied. The experiment was conducted in naturally sunlit, controlled environment Soil-Plant-Atmosphere-Research (SPAR) chambers at the Beltsville Agricultural Research Center, Beltsville, Maryland (Kim et al., 2006). The physical configuration of these chambers and methods of environmental control have been described by Baker et al. (2004).

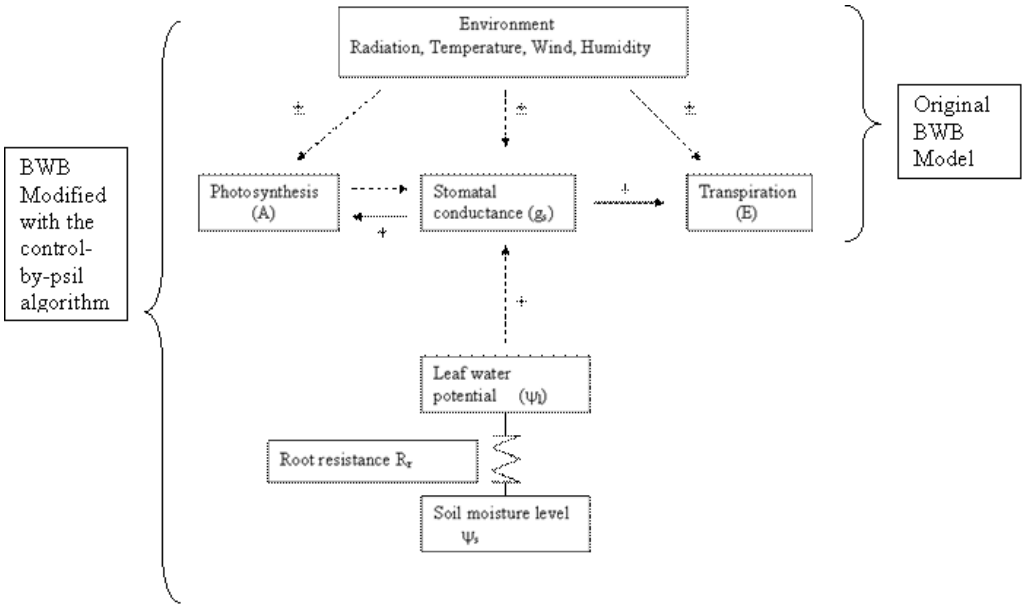

Figure 2. Interactions involved in control of stomatal conductance (g_s). In the original BWB model, g_s is assumed to be a function only of atmospheric environmental conditions and photosynthesis rate. In the BWB model modified by the control-by-psil algorithm, stomatal conductance is also a function of leaf water potential, which is hydraulically linked to soil water status. Therefore, stomatal conductance in the modified BWB model is also affected by soil moisture level. The "+" and "–" symbols indicate a process that is positively or negatively affected by the changes in environmental conditions or in another process.

Maize plants (*Zea mays* L. cv. Pioneer hybrid 34N43) were grown on a mixture of sterilized sand and vermiculite (1:1 by volume). Maize seed was sown on 28 May 2004. The initial plant density was 36 plants m^{-2}. The plants were thinned for destructive harvests over a period of two weeks beginning when the plants were at V-4. The final plant density in each chamber was maintained at 12 plant m^{-2} from about V-5 or V-6 onward. Transpiration and photosynthesis rates of all the plants in a chamber were measured and recorded. Since the simulated transpiration and photosynthesis rates were those of a single plant, the measured data were scaled by the number of plants in the chamber to make sure that the measured data and simulation were comparable.

Data from three chambers with different water supply regimes were chosen for analysis. In all three chambers, photosynthetically active radiation (PAR) levels inside and outside the chambers were measured with quantum sensors (LI-190SB, LI-COR, Inc., Lincoln, Neb.). The atmospheric CO_2 level was controlled at 370 μmol mol^{-1} during daytime. During the experiment, air temperature inside the chambers was set to 27°C/27°C (day/night) early in the experiment. When plants grew to stage V16 to V17, air temperature was set to 27°C/16°C. The water supply treatment of each chamber was not altered during the experiment. Constant horizontal wind speed of 1.5 m s^{-1} was maintained in all chambers. Relative humidity inside the chambers was monitored but not controlled. Irrigation was provided by drippers arranged in three 2.0 m rows with an approximate spacing between rows of 0.20 m. Irrigation was varied in each of the chamber. The fully irrigated treatment was irrigated to fully replace water lost by evapotranspiration (ET). The "50%" treatment was fully irrigated until 39 days after emergence (DAE), and then irrigation was withheld. Irrigation in the "25%" treatment chamber was withheld for most of the time from the beginning of the experiment; when the plants were re-irrigated, the irrigation rates were lower than in the control chamber (fig. 3).

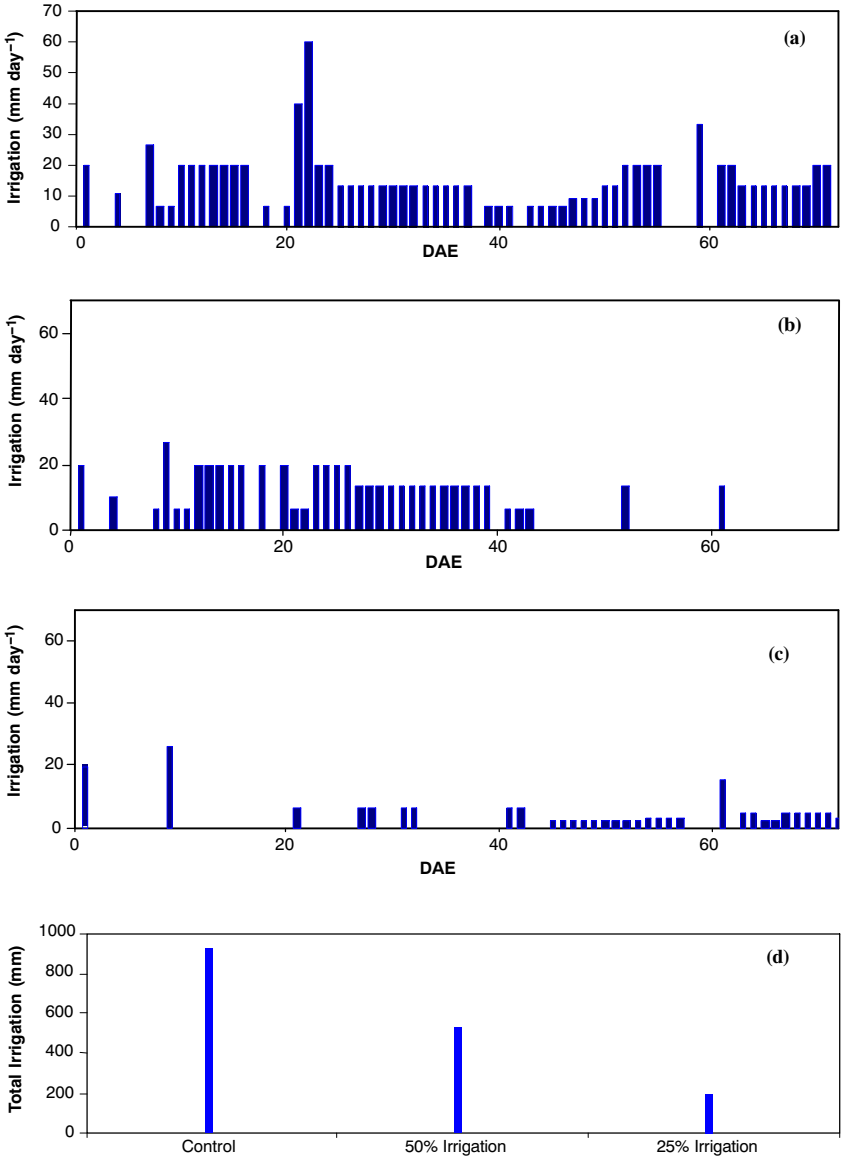

Figure 3. Daily irrigation rate in the (a) control, (b) 50% treatment, and (c) 25% treatment, and (d) the total amount of irrigation in each chamber during the experiment.

For each chamber, soil volumetric water content was recorded by fifteen TDR waveguides installed at five depths, replicated at three horizontal positions (Timlin et al., 2007). Water uptake was calculated from the TDR measurements by multiplying the volume of soil by water content and summing over the layers. Condensate was collected from the cooling coils of each chamber and weighed every 15 min (Timlin et al., 2007; Baker et al., 2004). This condensate was assumed to represent whole-canopy transpiration.

The CO_2 concentration of the air of each chamber was measured continuously with a dedicated infrared gas analyzer (LI-6252, LI-COR, Inc., Lincoln, Neb.). Medical-grade CO_2 from a compressed gas cylinder was used as the CO_2 supply source. Mass flow controllers (FMA-766-V-CO2, Omega Engineering, Inc. Stanford, Conn.) were used to regulate the injection rates of CO_2 with a feed-forward, feed-back proportional-integral-differential (PID) control algorithm. Canopy CO_2 exchange rates (CER) were calculated from mass balance equations and averaged and recorded every 5 min. Chamber CO_2 leakage rates were also determined daily using a N_2O drawdown method (Baker et al., 2004). The leakage rates were then used to correct CER for chamber leakage. From measured CER and chamber leakage rate, gross photosynthesis rates were calculated with the method described by Fleisher et al. (2006). Other environmental conditions, including relative humidity of the air, maximum/minimum temperature during the day, and wind velocity, were also measured. The soil hydraulic properties for the soils (van Genuchten, 1980) in all the chambers were fit from simulations during the first 30 days for the well irrigated chamber.

Diurnal and daily total canopy transpiration and photosynthesis rates were calculated from both measured and simulated data. To evaluate the performance of the coupled model with different stomatal controlling algorithms in simulating the transpiration and photosynthesis rate of the plants under different water treatments, measured leaf area index (LAI) values were applied in the simulations. The coefficient of correlation between simulation and measurements, the root mean square error (RMSE), and the relative error (RE) of the simulations were calculated:

$$\mathrm{RMSE} = \left[\frac{1}{n}\sum_{i=1}^{n}(\mathrm{Simulation}_i - \mathrm{Observation}_i)^2\right]^{1/2} \quad (6)$$

$$\mathrm{RE} = \mathrm{RMSE}/\mathrm{Measured\ average} \quad (7)$$

Results

Trends in Soil Water Content

The total irrigation for the season was 925, 530, and 200 mm, respectively, in the fully irrigated, 50% treatment, and 25% treatment chamber (fig. 3d). Difference in irrigation treatment resulted in different soil moisture status in the SPAR chambers (fig. 4). The coupled soil-plant-atmosphere model was able to simulate these differences and the general trend in soil moisture status (fig. 4). For the fully irrigated treatment (fig. 4a), the simulated water content at 5 to 30 cm started between 0.1 and 0.2 $cm^3\ cm^{-3}$ and quickly stabilized around 0.25 $cm^3\ cm^{-3}$ by DAE 10. The simulated water contents at 50 and 75 cm were maintained relatively stable around 0.3 and 0.4 $cm^3\ cm^{-3}$, respectively. The fluctuation in water content at 5 to 30 cm between DAE 20 and DAE 21, the decrease in water content at all depths from DAE 35 to DAE 40, and the increase in water content at all depths between DAE 40 to DAE 45 were all simulated by the model. The Pearson correlation coefficient (r) between measurement and simulation was 0.77, and the RMSE was 0.037. For the 50% treatment, simulated water content was between 0.2 and 0.3 $cm^3\ cm^{-3}$ at 5 to 50 cm and 0.4 $cm^3\ cm^{-3}$ at 75 cm until DAE 39. After DAE 39, simulated water content at all depths decreased continuously. At the end of simulation, water contents at depths of 5 to 30 cm, 50 cm, and 75 cm were around 0.1, 0.12, and 0.15 $cm^3\ cm^{-3}$, respectively. The fluctuation in water content caused by irrigation between DAE 20 to 23 and DAE 60 to 61 was well predicted by the model (fig. 4b). The Pearson correlation coefficient (r) between measurement and simulation and RMSE of the simulation for this treatment were 0.95 and 0.066, respectively. Simulated water content for the 25% treatment decreased at all depths from the beginning of simulation. At the end of simulation, water contents at all depths were lower than 0.15 $cm^3\ cm^{-3}$. The fluctuation in water content caused by irrigation and water uptake at 5 cm was simulated by the model throughout the experiment (fig. 4c). Values of correlation coefficient and RMSE were 0.93 and 0.054, respectively, for this treatment.

Trends in Transpiration and Photosynthesis

The coupled model was able to simulate the diurnal change in transpiration under different irrigation treatments. The measured diurnal changes in transpiration also reflected the difference in irrigation treatments. For the fully irrigated chamber, the model with and without a control algorithm simulated the diurnal change in transpiration equally well on DAE 30 (RMSE = 0.13) and DAE 56 (RMSE = 0.16) (figs. 5a and 5b). For the 50% treatment chamber, simulations with the two algorithms were identical and agreed with the measurement well on DAE 30 (fig. 5c, RMSE = 0.15). On DAE 56, simulations with the control-by-psil algorithm agreed with the measurements better than the no-control algorithm (fig. 5d, RMSE = 0.16 vs. RMSE = 0.18). For the 25% treatment, simulations with the control-by-psil algorithm performed better than the no-control algorithm on both DAE 30 (fig. 5e, RMSE = 0.16 vs. RMSE = 0.22) and DAE 56 (fig. 5f, RMSE = 0.16 vs. RMSE = 0.19).

Measured daily transpiration and photosynthesis throughout the experiment from each chamber also reflected the difference in irrigation treatments (figs. 6a through 6f), and the coupled MaizSim+2DSOIL model was able to simulate the general trend in the change of daily transpiration rate of plants under different irrigation treatments (figs. 6a through 6c). For the drought-stress treatment chambers, the model with the control-by-psil algorithm simulated the transpiration measurement better than the model with the no-control algorithm. As the drought stress became more severe, the improvement in simulation by the control-by-psil algorithm was more obvious (table 1).

When simulating the transpiration rate in the fully irrigated chamber, results by both algorithms agreed with the measurements well (fig. 6a). The simulated transpiration rates increased steadily and reached 44 mol H_2O $plant^{-1}$ day^{-1} by DAE 35. Afterward, simulated transpiration was maintained between 35 and 50 mol H_2O $plant^{-1}$ day^{-1} most of the time until the end of the simulation, except for a couple

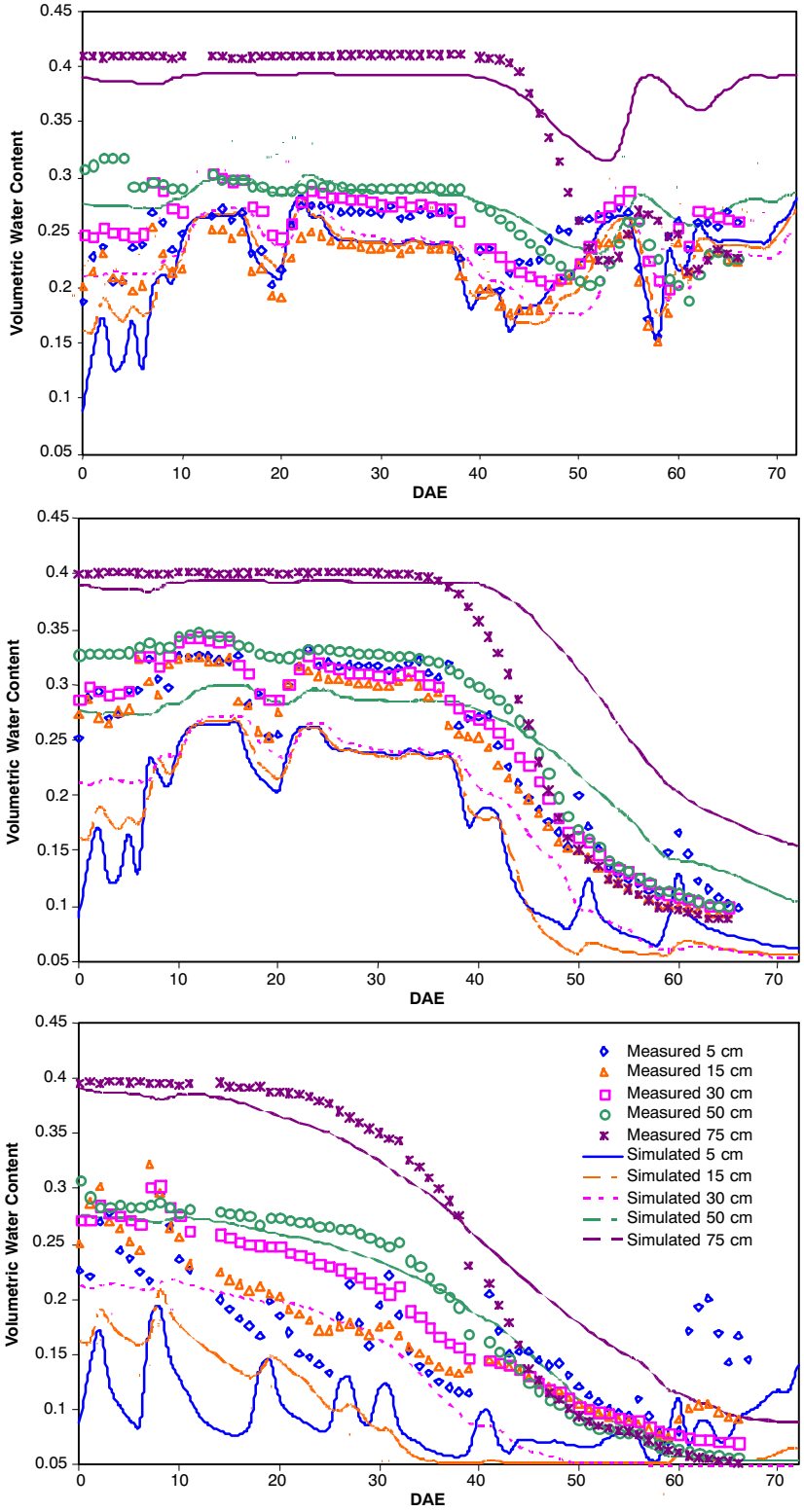

Figure 4. Soil volumetric water content in the chambers. Bottom soil layer in all three chambers was saturated at 0.4 since the bottom boundary of the soil bin was open to the atmosphere (Timlin et al., 2007).

of days during which there were low light levels (i.e., DAE 33 and 54).

When simulating the ET rate for the 50% treatment, the simulations with the control-by-psil algorithm were closer to the measurements than the no-control approach (fig. 6b). Both the RMSE and RE of the control-by-psil algorithm were lower (table 1). Figure 6b shows that, from DAE 1 to DAE 35, there were no obvious differences between transpiration simulated by the two approaches, and both approaches followed the general trend of increasing in transpiration quite well, although both slightly underestimated transpiration from DAE 1 to DAE 20 and overestimated the transpiration rate from

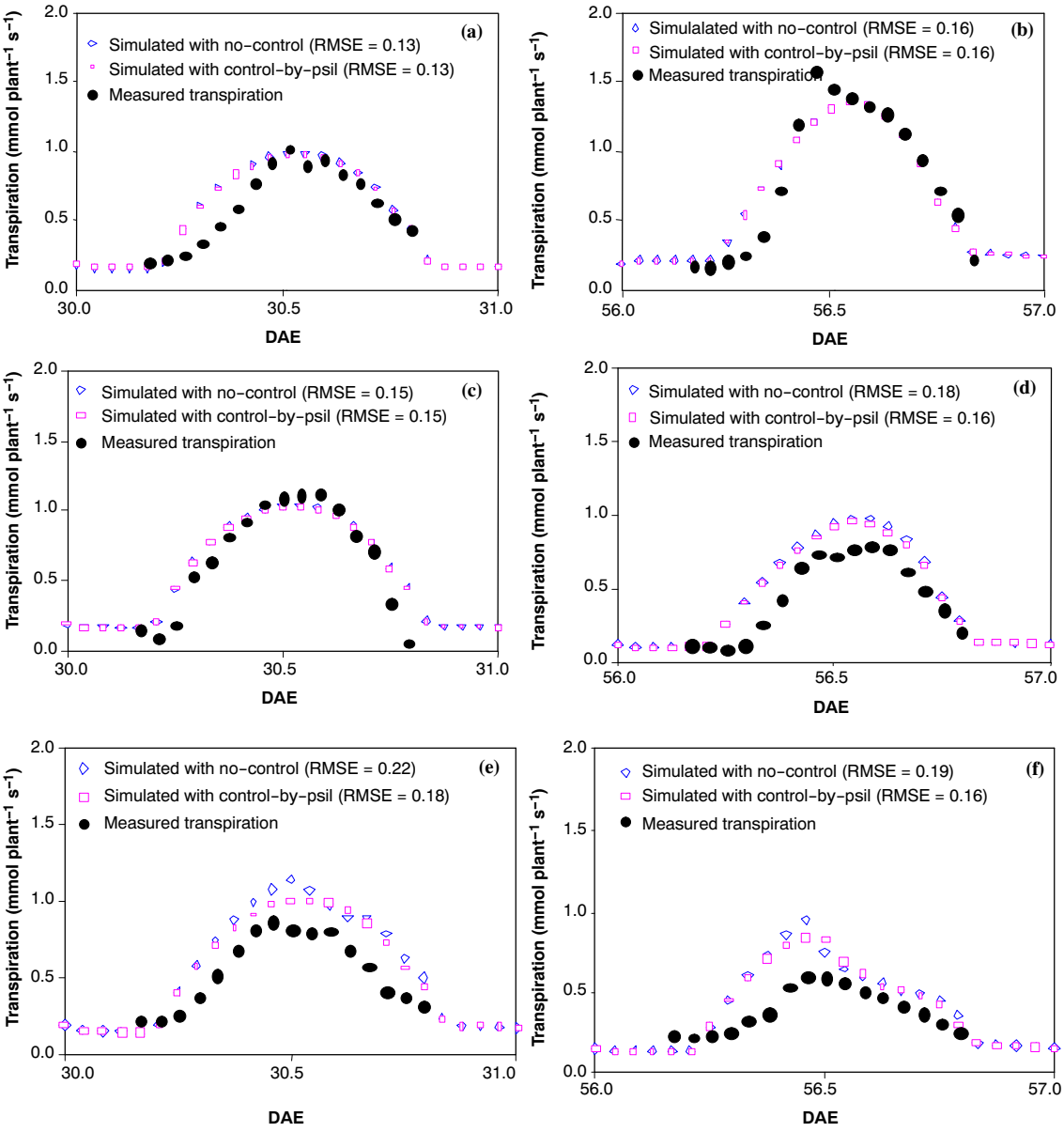

Figure 5. Diurnal changes in light level and VPD on (a) DAE 30 and (b) DAE 56, and diurnal change in transpiration rates of (c, d) fully irrigated, (e, f) 50% treatment, and (g, h) 25% treatment chambers, respectively, on DAE 30 and DAE 56.

DAE 20 to DAE 35. The plateau in transpiration rates and later decrease were well simulated by the model with either approach. Also worth noting was that from DAE 43 to DAE 58 (when the irrigation was withheld), the transpiration rates simulated with the control-by-psil algorithm were slightly lower than those simulated with no-control and closer to the measurements.

For the 25% treatment chamber, the simulated ET rates were lower than the simulations of the fully irrigated chamber throughout the experiment. The coupled model with either approach was also able to reproduce the general trend in the measurement (fig. 6c). The RE values (table 1) show that the model did not perform as well as it did in the treatments receiving full irrigation, but was comparable with the simulation for the 50% treatment. The control-by-psil algorithm was better than the no-control approach, judging by the lower RMSE. From figure 6c it can be observed that the ET rate simulated with the control-by-psil algorithm was lower than the simulations using no-control and was closer to the measurements most of the time during the experiment. After DAE 50, when the plants were re-irrigated, there were no obvious differences among simulated ET rates.

The coupled model was also able to simulate the general trend in photosynthesis rates under the contrasting water regimes. For the fully irrigated treatment (fig. 6d), the simulated photosynthesis rate increased steadily to 270 mmol CO_2 $plant^{-1}$ day^{-1} on DAE 35 and was maintained between 150 and 350 mmol CO_2 $plant^{-1}$ day^{-1} until the end of the simulation. Figure 6d also shows that there were no differences in the simulations between the photosynthesis rates simulated with different stomatal control algorithms.

For the 50% treatment, the simulated photosynthesis rates followed the measurements and increased to 250 mmol CO_2 $plant^{-1}$ day^{-1} by DAE 35. Between DAE 36 and DAE 50, the measured photosynthesis rate fluctuated between 150 and 350 mmol CO_2 $plant^{-1}$ day^{-1}, and the model was able to sim-

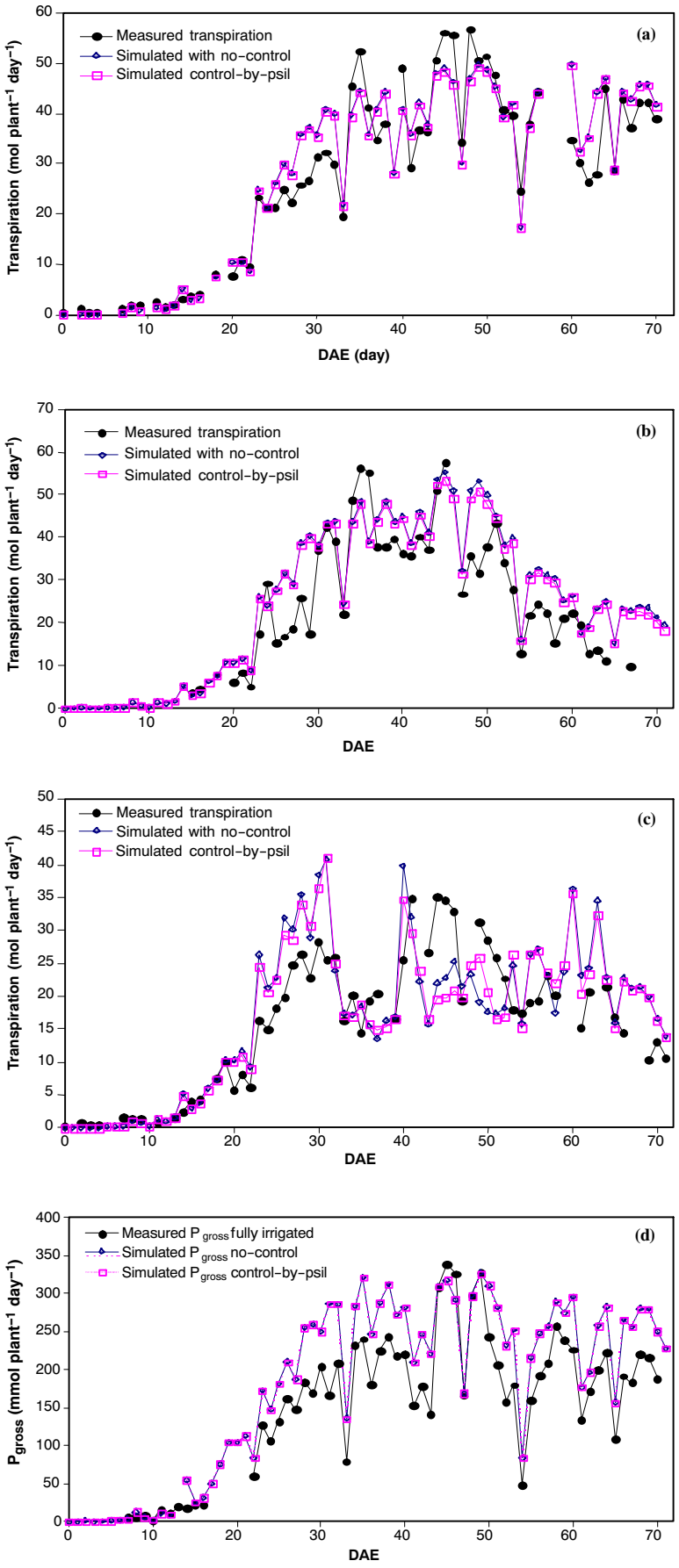

Figure 6(a–d). Measured and simulated transpiration and photosynthesis rate in the chambers.

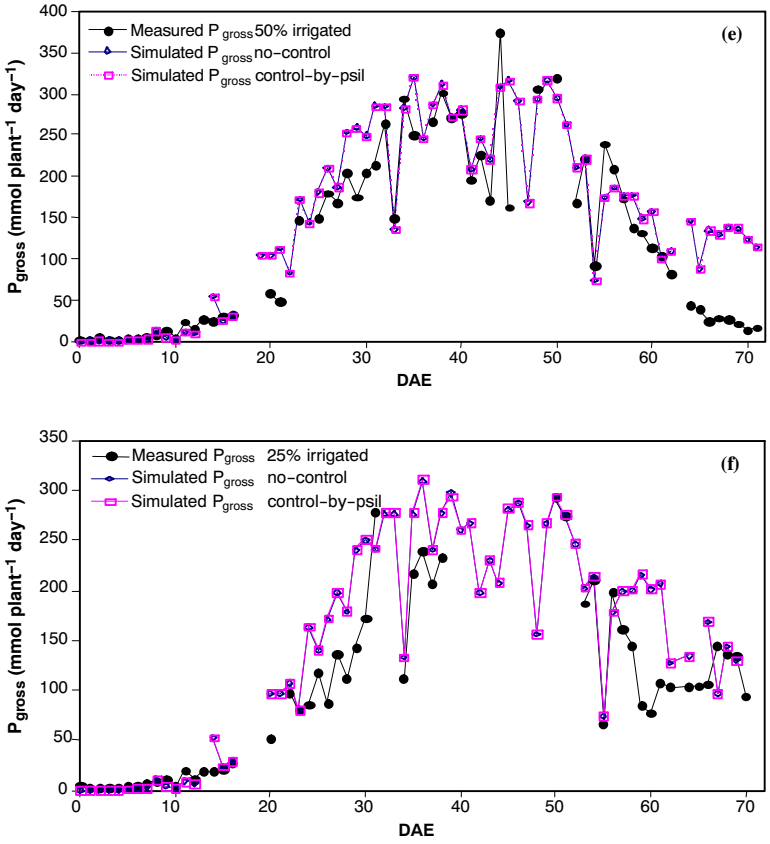

Figure 6(e-f). Measured and simulated transpiration and photosynthesis rate in the chambers.

Table 1. RMSE and RE (in parentheses) of the model with different stomatal control algorithms in transpiration simulation.

	Control		50% Irrigation		25% Irrigation	
	RMSE (RE)	r	RMSE (RE)	r	RMSE (RE)	r
No stomatal control	5.5 (0.17)	0.93	9.6 (0.34)	0.86	6.7 (0.36)	0.67
Controlled by psil signal	5.5 (0.17)	0.93	9.2 (0.32)	0.87	5.7 (0.30)	0.73

Table 2. RMSE (and RE) values of the model with different stomatal control algorithms in photosynthesis simulation.

	Control	50% Irrigation	25% Irrigation
No stomatal control	55.8 (0.34)	47.2 (0.34)	60.4 (0.34)
Stomata control by psil signal	55.8 (0.34)	47.2 (0.34)	61.0 (0.34)

ulate this plateau. After DAE 50, both the measured and the simulated photosynthesis rates decreased steadily. However, from DAE 60 to DAE 70, the simulations did not decrease as steadily as the measurements, so simulations in the last several days overestimated the photosynthesis rate. Like the simulation in the fully irrigated chamber, no differences were observed among the simulations with different control mechanisms.

For the 25% treatment, the coupled model was able to simulate the general trend, increasing to 260 mmol CO_2 plant^{-1} day^{-1} by DAE 35, maintaining around 130 to 310 mmol CO_2 plant^{-1} day^{-1} between DAE 36 and DAE 50, and then decreased steadily to 100 mmol CO_2 plant^{-1} day^{-1} at the end of simulation. From DAE 51 to DAE 65, the simulations overestimated the measured photosynthesis rate by an average of 144.3 mmol CO_2 plant^{-1} day^{-1}. Simulations with both algorithms were identical.

The RMSE and RE of the photosynthesis simulations are listed in table 2. Values in the table show that the simulations of photosynthesis using the model with both stomatal control algorithms were identical under different water regimes.

Discussion

In the coupled model, the simulated transpiration rates were not only determined by atmospheric demand (figs. 1 and 2), but also by soil water content and stomatal conductance. When stomatal closure was linked to soil water status, stomatal conductance was reduced as the amount of soil water was reduced. The lower stomatal conductance resulted in a reduced transpiration rate. The lowered transpiration rate helped to maintain leaf water potential, so the leaf water potential simulated with a controlling algorithm was higher than that simulated without a controlling algorithm (Tardieu and Simonneau, 1998).

For the fully irrigated chamber, the soil water content was consistently maintained at high levels during the experiment, so the stomatal conductance simulated with the control-by-psil algorithm was very close to that simulated with the no-control approach. Because transpiration demand and amount of irrigation water were also the same for both approaches in

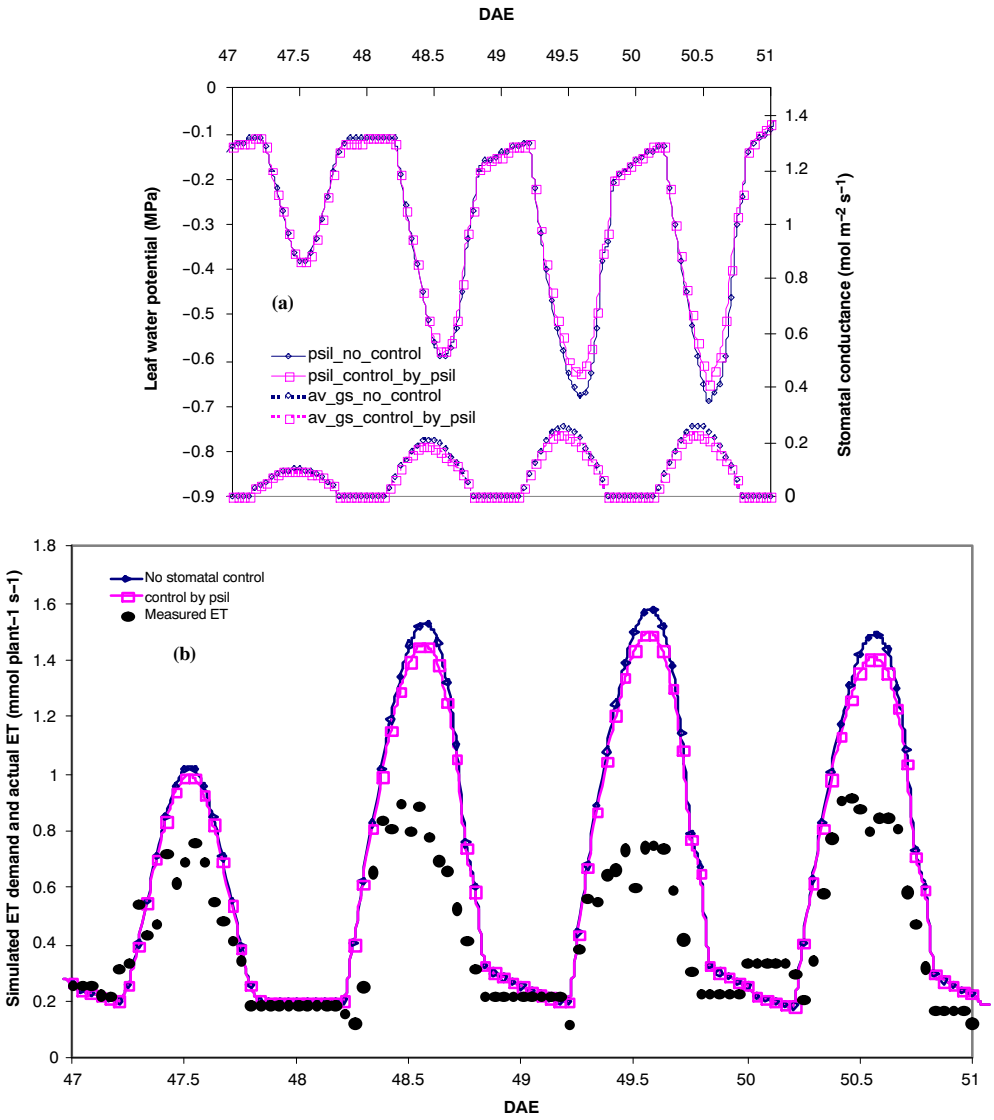

Figure 7. Simulation of (a) leaf water potential and stomatal conductance, and (b) ET demand from DAE 47 to DAE 51 in the 50% treatment chamber.

the simulations, the diurnal change and daily transpiration rates simulated with the different algorithms were very similar to each other.

For the 50% treatment, water was not withheld until DAE 39. Up to this day, soil water content was kept at similar level to those of the fully irrigated treatment. Therefore, the simulated leaf water potential and stomatal conductance, and the measured and simulated transpiration rates, were similar to those of the fully irrigated treatment. After irrigation was withheld, soil water content decreased more than 40% from DAE 47 to DAE 51 (fig. 4b). The simulated leaf water potential decreased during the same period. Figure 7 also shows that as drought stress developed, the stomatal conductance simulated with the control-by-psil algorithm became lower than that simulated with the no-control algorithm (fig. 7a), resulting in lower transpiration demand under the same atmospheric condition (fig. 7b). The lower transpiration demand helped to maintain the smaller drop in leaf water potential than that simulated without control (fig. 7a) and ultimately a lower simulated transpiration rate, which was closer to the observation. This explains why the control-by-psil algorithm performed better than the no-control algorithm in simulating transpiration when drought stress developed.

For the 25% treatment chamber, the soil water content decreased continuously (fig. 4). The leaf water potential simulated with no stomatal control was driven lower by the decreasing soil moisture and the increasing transpiration demand as the plant developed. On DAE 26, the leaf water potential simulated with no control reached −1.2 MPa (fig. 8a). The simulated leaf water potential with the control-by-psil algorithm also decreased continuously. The decreased leaf water potential resulted in lower stomatal conductance, so the transpiration demand became lower than that simulated using no control (fig. 8b). The leaf water potential needed to satisfy the lowered ET demand therefore was not as low as that simulated with no stomatal control.

In the simulations, the reference leaf water potential in the control-by-psil algorithm was set to −1.2 MPa (Tuzet et al., 2003). Therefore, any leaf water potential lower than this value will result in a much lower stomatal conductance value than that simulated with the no-control approach. Depending on the sensitivity of stomata to leaf water potential, the reference leaf water potential ranges from −1.2 to −2.6 MPa (Henson et al., 1989; Leuning et al., 2003). A lower reference value means that the plant is more tolerant of water stress. Ac-

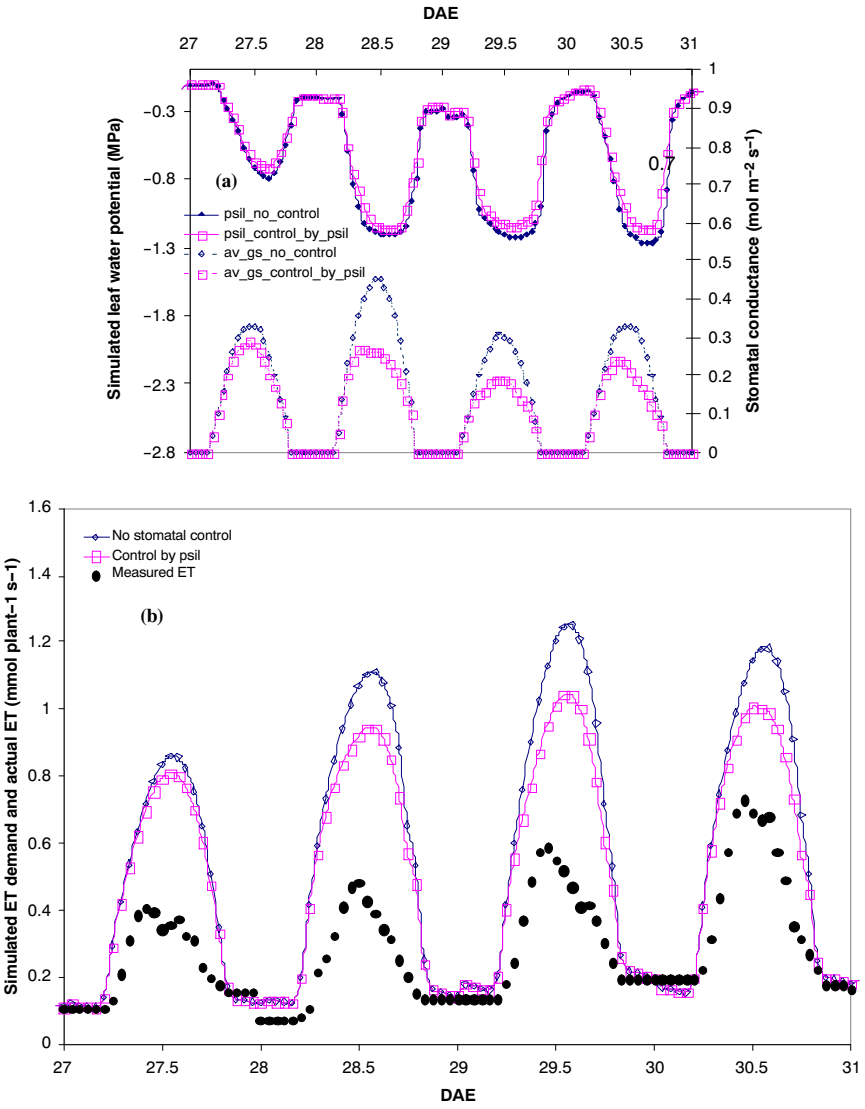

Figure 8. Simulation of (a) leaf water potential and stomatal conductance, and (b) ET demand from DAE 27 to DAE 31 in the 25% treatment chamber.

cording to Tuzet et al. (2003), corn, as an "isohydric" plant, should have high stomatal sensitivity to leaf water potential. Using different reference values in the control-by-psil algorithm enabled the stomatal conductance model to explain the behavior of stomata in terms of stomatal sensitivity to leaf water potential, without explicatively invoking hormonal control.

Water stress in corn results in smaller leaves and early leaf senescence (Boyer, 1970; Tanguilig et al., 1987; Granier and Tardieu, 1999). Smaller leaf area means less intercepted light, and thus lower transpiration demand. At the end of the experiment, severe drought stress caused leaf rolling, drooping, and wilting, which was not accounted for in the measured leaf area index (LAI). This may have been one of the main reasons the model overestimated transpiration and photosynthesis late in the season for both the 50% and 25% treatments.

The model also overestimated photosynthesis rate late in the experiment (figs. 6d through 6f). Considering that transpiration was also overestimated in this period, it may be concluded that the model overestimated light interception. Further studies should be conducted to search for better ways to quantitatively describe the effect of leaf rolling, drooping, and wilting on light interception, transpiration, and photosynthesis.

We also observed that the simulated photosynthesis was not as sensitive to the decrease in stomatal conductance as the simulated transpiration. This was a direct result of the way the stomatal conductance and photosynthesis modules in the model were solved to determine stomatal conductance as well as photosynthesis. Because of the complexity of the functions in the modules, a numerical methodology was adopted to search for the value of internal CO_2 concentration (C_i) in the modules iteratively. During the numerical search, a C_i value was determined at the point where the CO_2 supply rate (the CO_2 supply line in fig. 9) equaled the CO_2 demand rate (the A/C_i curve in fig. 9). In this study, it was noted that the value of the simulated C_i in the C_4 photosynthesis model was mostly kept above 150 µbar. The simulated photosynthesis rates were therefore at the horizontal portion of the A/Ci curve (fig. 9), and thus the changes in the stomatal conductance did not have strong effects on the simulated CO_2 assimilation rate. This insensitivity of photosynthesis to decrease

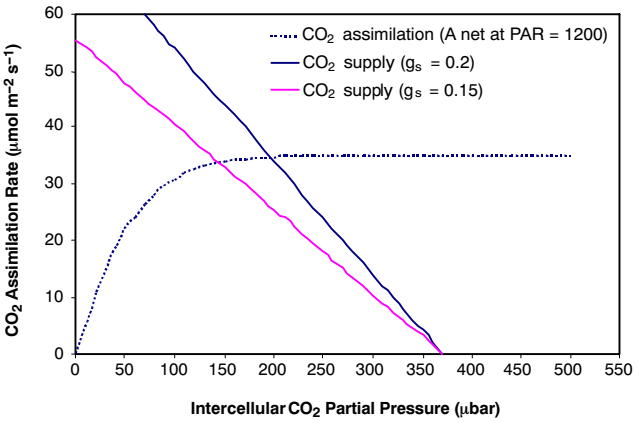

Figure 9. CO_2 assimilation rate as a function of CO_2 partial pressure when PAR = 1200 μmol m^{-2} s^{-1} and g_s = 0.15 and 0.2 μmol m^{-2} s^{-1}. Since the simulated photosynthesis rate is on the plateau of the A/C_i curve, the change in gs does not change CO_2 assimilation rate.

in stomatal conductance agrees with finding by Barradas and Jones (1996) and Jones (1998). Pachepsky and Acock (1996) and Parkhurst (1994) also reported that low stomatal conductance reduces water loss more than it reduces CO_2 uptake. Ferreyra et al. (2003) explained this phenomenon by the nonlinear relationship between the reactions of transpiration and photosynthesis to reducing stomatal conductance.

Conclusion

A soil-plant-atmosphere continuum model was constructed by coupling a corn model (MaizSim) and the 2DSOIL model in the effort to simulate transpiration and photosynthesis of corn under drought stress. A stomatal controlling algorithm (control-by-psil) was implemented in the coupled model and compared to a no-control approach. Transpiration and photosynthesis simulations were compared with measurements of corn plants under contrasting irrigation treatments.

The coupled model was able to simulate the changes in soil moisture level and the changes in transpiration and photosynthesis of corn plants under different water treatment regimes. The coupled model with a stomatal controlling mechanism performed better than that without stomatal control in simulating transpiration of corn plants on drying soil. When plants were well watered or under minor water stress, the improvement in simulation performance was not very significant. However, as water stress becomes more severe, the improvement became more obvious.

It was also observed that the simulated photosynthesis rates were not as sensitive to stomatal closure as simulated transpiration. The result agreed with the different sensitivity of photosynthesis and transpiration to changes in stomatal closure that have been reported and discussed in the literature.

These results suggest that the coupled model not only is a valuable tool for studying corn transpiration and photosynthesis under drought stress, but it also provides a platform to implement and evaluate algorithms in studies of corn crop water dynamics and CO_2 assimilation.

References

Acock, B., and A. Trent. 1991. *The Soybean Crop Simulator GLYCIM: Documentation for the Modular Version 91.* Moscow, Idaho: University of Idaho, Department of Plant, Soil and Entomological Sciences.

Aphalo, P. J., and P. G. Jarvis. 1993. An analysis of Ball's empirical model of stomatal conductance. *Ann. Botany* 72(4): 321-327.

Baker, J. T., S.-H. Kim, D. C. Gitz, D. J. Timlin, and V. R. Reddy. 2004. A method for estimating carbon dioxide leakage rates in controlled environment chambers using nitrous oxide. *Environ. Exp. Botany* 51(2): 103-110.

Ball, J. T., I. E. Woodrow, and J. A. Barry. 1987. A model predicting stomatal conductance and its contribution to the control of photosynthesis under different environmental conditions. In *Progress in Photosynthesis Research*, IV: 221-224. I. Biggins, ed. Dordrecht, The Netherlands: Martinus-Jijhoff.

Barradas, V., and H. G. Jones. 1996. Response of CO_2 assimilation to changes in irradiance: Laboratory and field data and a model for beans (*Phaseolus vulgaris* L.). *J. Exp. Botany* 47(5): 639-645.

Boyer, J. S. 1970. Leaf enlargement and metabolic rates in corn, soybean, and sunflower at various leaf water potentials. *Plant Physiol.* 46(2): 233-235.

Buckley, T. N., and K. A. Mott. 2002. Stomatal water relations and the control of hydraulic supply and demand. In *Progress in Botany*, 63: 309-325. New York, N.Y.: Springer.

Campbell, G. S., and J. M. Norman. 2000. *An Introduction to Environmental Biophysics.* 2nd ed. New York, N.Y.: Springer.

Collatz, G. J., J. T. Ball, C. Grivet, and J. A. Berry. 1991. Physiological and environmental regulation of stomatal conductance, photosynthesis, and transpiration: A model that includes a laminar boundary layer. *Agric. and Forest Met.* 54(2-4):107-136.

Cowan, I. R. 1977. Stomatal behaviour and environment. In *Advances in Botanical Research*, 4: 177-228. R. Preston and H. W. Woolhouse, eds. London, U.K.: Academic Press.

Dang, Q. L., H. A. Margolis, and G. J. Collatz. 1998. Parameterization and testing of a coupled photosynthesis-stomatal conductance model for boreal trees. *Tree Physiol.* 18(3): 141-153.

De Pury, D. G. G., and D. D. Farquhar. 1997. Simple scaling of photosynthesis from leaves to canopy without errors of big-leaf models. *Plant, Cell and Environ.* 20(5): 537-557.

Dewar, R. C. 2002. The Ball-Berry-Leuning and Tardieu-Davies stomatal models: Synthesis and extension within a spatially aggregated picture of guard cell function. *Plant, Cell and Environ.* 25(11): 1383-1398.

Ferreyra, R. A., J. L. Dardanelli, L. B. Rachepsky, D. J. Collino, P. C. Faustinelli, G. Giambastiani, V. R. Reddy, and J. W. Jones. 2003. Nonlinear effects of water stress on peanut photosynthesis at crop and leaf scales. *Ecol. Model.* 168(1-2): 57-76.

Fleisher, D. H., D. J. Timlin, and V. R. Reddy. 2006. Temperature influence on potato leaf and branch distribution and on canopy photosynthetic rate. *Agron. J.* 98(6): 1442-1452.

Gao, C., P. Zhao, X. Zeng, X. Cai, and W. Shen. 2002. A model of stomatal conductance to quantify the relationship between leaf transpiration, microclimate, and soil water stress. *Plant, Cell and Environ.* 25(11): 1373-1381.

Grams, T. E. E., C. Koziolek, S. Lautner, R. Matyssek, and J. Fromm. 2007. Distinct roles of electric and hydraulic signals on the reaction of leaf gas exchange upon re-irrigation in *Zea mays* L. *Plant, Cell and Environ.* 30(1): 79-84.

Granier, C., and F. Tardieu. 1999. Water deficit and spatial pattern of leaf development: Variability in responses can be simulated using a simple model of leaf development. *Plant Physiol.* 119(2): 609-619.

Henson, I. E., C. R. Jensen, and N. C. Turner. 1989. Leaf gas exchange and water relations of lupins and wheat: I. Shoot response to soil water deficit. *Australian J. Plant Physiol.* 16(5): 401-413.

Hirasawa, T., and T. C. Hsiao. 1999. Some characteristics of reduced leaf photosynthesis at midday in maize growing in field. *Field Crops Res.* 62(1): 53-62.

Jensen, C. R., S. E. Jacobsen, M. N. Andersen, N. Nunez, S. D. Andersen, L. Rasmussen, and V. O. Mogensen. 2000. Leaf gas exchange and water relation characteristics of field quinoa (*Chenopodium quinoa* Willd) during soil drying. *European J. Agron.* 13(1): 11-25.

Jones, H. G. 1998. Stomatal control of photosynthesis and transpiration. *J. Exp. Botany* 49(special issue): 387-398.

Kim, S. H., and J. H. Lieth. 2003. A coupled model of photosynthesis, stomatal conductance, and transpiration for a rose leaf (*Rosa hybrida* L.). *Ann. Botany* 91(7): 771-781.

Kim, S. H., R. C. Sicher, H. Bae, H. Gitz, D. C. Baker, D. J. Timlin, and V. R. Reddy. 2006. Canopy photosynthesis, evapotranspiration, leaf nitrogen, and transcription profiles of maize in response to CO_2 enrichment. *Global Change Biol.* 12(3): 588-600.

Leuning, R. 1995. A critical appraisal of a combined stomatal-photosynthesis model for C_3 plants. *Plant, Cell and Environ.* 18(4): 339-355.

Leuning, R., A. Tuzet, and A. Perrier. 2003. Stomata as part of the soil-plant-atmosphere continuum. In *Forests at the Land-Atmosphere Interface*, 9-29. M. Mencuccini, J. Grace, J. Moncrieff, and K. McNaughton, eds. Edinburgh, Scotland: CAB International.

Lhomme, J. P., E. Elguero, A. Chehbouni, and G. Boulet. 1998. Stomatal control of transpiration: Examination of Monteith's formulation of canopy resistance. *Water Resource Res.* 34(9): 2301-2308.

Malone, M., and B. Stankovic. 1991. Surface potentials and hydraulic signals in wheat leaves following localized wounding by heat. *Plant, Cell and Environ.* 14(4): 431-436.

Mercado, L., J. Lloyd, F. Carswell, Y. Malhi, P. Meir, and A. D. Nobre. 2006. Modelling Amazonian forest eddy covariance data: A comparison of big leaf versus sun/shade models for the C-14 tower at Manaus I. Canopy photosynthesis. *Acta Amazonica* 36(1): 69-82.

Pachepsky, L. B., and B. Acock. 1996. A model 2DLEAF of leaf gas exchange: Development, validation, and ecological application. *Ecol. Model.* 93: 1-18.

Parkhurst, D. F. 1994. Tansley Review No. 65: Diffusion of CO_2 and other gases inside leaves. *New Phytol.* 126(3): 449-479.

Pfeffer, M., and M. Peisker. 1998. CO_2 gas exchange and phosphoenolpyruvate carboxylase activity in leaves of *Zea mays* L. *Photosynthesis Res.* 58(3): 281-291.

Tanguilig, V. C., E. B. Yambao, J.C. O'Toole, and S. K. De Datta. 1987. Water stress effects on leaf elongation, leaf water potential, transpiration, and nutrient uptake in rice, maize, and soybean. *Plant and Soil* 103(2): 155-168.

Tardieu, F., and T. Simonneau. 1998. Variability among species of stomatal control under fluctuating soil water status and evaporative demand: Modelling isohydric and anisohydric behaviours. *J. Exp. Botany* 49(special issue): 419-432.

Timlin, D. J., Y. Pachepsky, and B. Acock. 1996. A design for a modular, generic soil simulator to interface with plant models. *Agron. J.* 88(2): 162-169.

Timlin, D. J., Y. Pachepsky, B. A. Acock, J. Simunek, G. Flerchinger, and F. Whisler. 2002. Error analysis of soil temperature simulations using measured and estimated hourly weather data with 2DSOIL. *Agric. Sys.* 72(3): 215-239.

Timlin, D. J., D. Fleisher, S-H. Kim, V. R. Reddy, and J. Baker. 2007. Evapotranspiration measurement in controlled environment chambers: A comparison between time domain reflectometry and accumulation of condensate from cooling coils. *Agron. J.* 99(1): 166-173.

Tuzet, A., A. Perrier, and R. Leuning. 2003. A coupled model of stomatal conductance, photosynthesis, and transpiration. *Plant, Cell and Environ.* 26(7): 1097-1116.

van Genuchten, M. Th. 1980. A closed-form equation for predicting the hydraulic conductivity of unsaturated soils. *SSSA J.* 44(5): 892-898.

Von Caemmerer, S. 2000. *Biochemical Models of Leaf Photosynthesis.* Collingwood, Australia: CSIRO Publishing.

Wei, C., M. T. Tyree, and E. Steudle. 1999. Direct measurement of xylem pressure in leaves of intact maize plants: A test of the cohesion-tension theory taking hydraulic architecture into consideration. *Plant Physiol.* 121(4): 1191-1205.

Williams, M., E. B. Rastetter, D. N. Fernandes, M. L. Goulden, S. C. Wofsy, G. R. Shaver, J. M. Melillo, J. W. Munger, S.-M. Fan, and K. J. Nadelhoffer. 1996. Modelling the soil-plant-atmosphere continuum in a *Quercus acer* stand at Harvard Forest: The regulation of stomatal conductance by light, nitrogen and soil/plant hydraulic properties. *Plant, Cell and Environ.* 19(8): 911-927.

Yao, C., S. Moreshet, and B. Aloni. 2001. Water relations and hydraulic control of stomatal behaviour in bell pepper plant in partial soil drying. *Plant, Cell and Environ.* 24(2): 227-235.

APPENDIX A

C_4 PHOTOSYNTHESIS MODEL AND SIMULATION FOR TRANSPIRATION DEMAND

In the coupled model, the net canopy photosynthesis (A) is determined using the biochemical model of C_4 photosynthesis of Von Caemmerer (2000). In the model, CO_2 assimilation is limited either by Rubisco activity or by electron transport. Net photosynthesis is expressed as:

$$A = \min\left\{A_c, A_j\right\} \tag{A1}$$

$$A_c = \min\left\{\left(V_p + g_s C_m - R_m\right)\left(V_{c\max} - R_d\right)\right\} \tag{A2}$$

$$A_j = \min\left\{\left(\frac{xJ}{2} + g_{bs}C_m - R_m\right)\left(\frac{(1-x)J}{3} - R_d\right)\right\} \tag{A3}$$

where x is the partitioning factor of electron transport rate between C_3 and C_4 cycles (= 0.4).

$$V_p = V_{p\max}\frac{C_m V_{p\max}}{C_m + K_p} \tag{A4}$$

where K_p is the Michaelis-Menten constant for CO_2 of PEPC and was set to 57.0 μmol mol^{-1} (Pfeffer and Peisker, 1998).

$$\theta J^2 - J\left(I_2 + J_{\max}\right) + I^2 J_{\max} = 0 \tag{A5}$$

where θ is an empirical curvature factor (= 0.7).

$$g(T_k) = k_{25}\exp\left[\frac{E_a(T_k - 298)}{298RT_k}\right]\frac{\left[1+\exp\left(\frac{298S - H}{298R}\right)\right]}{\left[1+\exp\left(\frac{ST_k - H}{RT_k}\right)\right]} \tag{A6}$$

The transpiration demand is determined as:

$$E = 2g_v\left(\frac{e_s(T_L) - e_a}{P_a}\right) \quad \text{(A7)}$$

where E is transpiration demand (mol m^{-2} s^{-1}), g_v is total water vapor conductance per surface leaf area (mol m^{-2} s^{-1}), e_a is water vapor pressure of the air (kPa), P_a is atmospheric pressure (kPa), T_L is leaf surface temperature, and $e_s(T_L)$ is saturated water vapor pressure (definitions of all parameters are presented in Appendix B).

$$e_s(T) = 0.611\exp\left(\frac{17.502T}{240.97 + T}\right) \quad \text{(A8)}$$

$$T_L = T_a + \frac{R_{abs} - \varepsilon\sigma T_a^4 - \lambda g_v D / P_a}{c_p(g_h + g_r) + \lambda\left(\left(de_s(T_a)/dT\right)/P_a\right)g_v} \quad \text{(A9)}$$

where T_a is air temperature (°C), R_{abs} is absorbed longwave and shortwave radiation per surface leaf area (W m^{-2}), ε is leaf thermal emissivity (= 0.97), σ is the Stefan-Boltzmann constant (5.67 × 10^{-8} W m^{-2} K^{-4}), λ is latent heat of vaporization at 25°C (= 44.0 J mol^{-1} °C^{-1}), c_p is specific heat of air (= 29.3 J mol^{-1} °C^{-1}), D is vapor pressure deficit of ambient air (kPa), g_h is heat conductance for the boundary layer per leaf surface area (mol m^{-2} s^{-1}), and g_r is radiative conductance per surface leaf area (mol m^{-2} s^{-1}) (Campbell and Norman, 2000).

$$g_h = \frac{0.135}{0.147}g_b \quad \text{(A10)}$$

where g_b is boundary layer conductance to water vapor:

$$g_b = 0.147\sqrt{\frac{u}{d}} \quad \text{(A11)}$$

where u is wind speed, and d is the characteristic leaf dimension of a leaflet in relation to width (w):

$$d = 0.72w \quad \text{(A12)}$$

$$g_r = \frac{4\varepsilon\sigma T_L^3}{c_P} \quad \text{(A13)}$$

$$g_v = 0.5\frac{g_s g_b}{g_s + g_b} \quad \text{(A14)}$$

where g_s is stomatal conductance to water vapor (mol m^{-2} s^{-1}).

Appendix B

Symbols, Parameters, and Their Values Used in the Simulation

A = net CO_2 assimilation rate (μmol m^{-2} s^{-1})
A_c = Robisco-limited CO_2 assimilation (μmol m^{-2} s^{-1})
A_j = electron-transport-limited rate of CO_2 assimilation (μmol m^{-2} s^{-1})
c_p = specific heat of air (29.3 mol^{-1} °C^{-1})
d = characteristic leaf dimension of a leaflet in relation to width
C_s = CO_2 partial pressure at the leaf surface (μbar)
C_m = mesophyll CO_2 partial pressure (μbar)
D = vapor pressure deficit of the ambient air (kPa)
E = transpiration demand (mol m^{-2} s^{-1})
e_a = vapor pressure in the air (kPa)
$e_s(T_L)$ = saturated water vapor pressure (kPa)
g_v = total water vapor conductance per surface leaf area (mol m^{-2} s^{-1})
g_h = heat conductance for boundary layer per leaf surface area (mol m^{-2} s^{-1})
g_r = radiative conductance per surface leaf area (mol m^{-2} s^{-1})
g_b = boundary layer conductance to water vapor (mol m^{-2} s^{-1})
g_s = stomatal conductance to water vapor (mol m^{-2} s^{-1})
g_0 = minimum stomatal conductance to water vapor at the light compensation point in the BWB model (0.096 mol m^{-2} s^{-1})
g_1 = empirical coefficient for the sensitivity of g_s to A, C_s, and h_s (10.055)
h_s = relative humidity at the leaf surface
I_2 = photosynthetically active irradiance absorbed by PS II (μmol quanta m^{-2} s^{-1})
I = incident irradiance (μmol quanta m^{-2} s^{-1})
J_w = actual water uptake rate (mol H_2O m^{-2} s^{-1})
J = electron transport rate (μmol electrons m^{-2} s^{-1})
J_{max} = maximal electron transport rate (μmol electrons m^{-2} s^{-1})
K_p = Michaelis-Menten constant for CO_2 of PEPC (57 μmol mol^{-1})
P_a = atmospheric pressure (kPa)
R_{abs} = absorbed longwave and shortwave radiation per surface leaf area (W m^{-2})
R_d = mitochondrial respiration in the light (μmol m^{-2} s^{-1})
R_m = mitochondrial respiration in the mesophyll (μmol m^{-2} s^{-1})
R_r = root hydraulic resistance (m^2 s MPa/mol H_2O)
R_{sr} = soil to root hydraulic resistance (m^2 s MPa/mol H_2O)
R_z = xylem hydraulic resistance (149 m^2 s MPa/mol H_2O)
s_f = sensitivity parameter (2.3)
T_a = air temperature (°C)
u = wind speed (m s^{-1})
V_w = partial molar volume of water (0.000018)
V_p = PEP carboxylation rate (μmol m^{-2} s^{-1})
V_{cmax} = maximal Rubisco carboxylation rate (μmol m^{-2} s^{-1})
V_{pmax} = maximal PEP carboxylation rate (μmol m^{-2} s^{-1})
x = partitioning factor of electron transport rate between C_3 and C_4 cycles (0.4)
δ = sensitivity coefficient (-1 MPa^{-1})
ε = leaf thermal emissivity (0.97)
λ = latent heat of vaporization at 25°C (44 J mol^{-1} °C^{-1})
θ = empirical curvature factor (0.7)
σ = Stefan-Boltzmann constant (5.67 × 10^{-8} W m^{-2} K^{-4})
ψ_l = bulk leaf water potential (MPa)
ψ_f = reference bulk leaf water potential (–1.2 MPa)
ψ_s = soil water potential (MPa)